Stochasticity in the Switching of Nanodisks for Probabilistic Computing

Hee-Sung Han,[†, ‡, ¶] *Sooseok Lee,*[‡, ¶] *Soong-Geun Je,*[§] *Myeonghwan Kang,*[‡] *Hye-Jin Ok,*[‡] *Namkyu Kim,*[‡] *Weilun Chao,*[†] *Mi-Young Im*[*, †] *and Ki-Suk Lee,*[*, ‡]

[†]Center for X-ray Optics, Lawrence Berkeley National Laboratory, Berkeley, CA94720, USA.

[‡]Department of Materials Science and Engineering, Ulsan National Institute of Science and Technology, Ulsan 44919, Republic of Korea.

[§]Department of Physics, Chonnam National University, Gwangju 61186, Republic of Korea.

*Correspondence to Mi-Young Im (mim@lbl.gov) and Ki-Suk Lee (kisuk@unist.ac.kr).

[¶]Hee-Sung Han and Sooseok Lee contributed equally to this work.

Abstract

Stochasticity in magnetic nanodevices is an essential characteristic for harnessing those devices to computing based on population coding or the building blocks of probabilistic computing, p-bits. A magnetic tunneling junction (MTJ) consisting of a patterned magnetic element is considered as a promising computing unit in the concept of artificial neurons and p-bits. The comprehensive understanding of the stochasticity in the switching of patterned magnetic elements is crucial for realizing MTJ based probabilistic computing technology. In the present work, the stochastic behavior in switching process of a perpendicularly magnetized Co/Pt disk within an array was directly observed utilizing full-field soft X-ray microscopy. Within 50 repeated hysteretic cycles, the stochastic magnetization switching of individual Co/Pt disks within disk arrays is identified. We found that the stochasticity in the magnetization switching of disks considerably depends on the disk size. The stochasticity initially decreases as the disk radius gets bigger from 125 nm to 375 nm (Region I), then increases with further enlarging disk size to 625 nm (Region II). The variance of thermal fluctuation relevant to the disk size and the multi-level switching within a disk are severely involved in the observed size dependent stochasticity. This work provides the way for controlling the stochasticity in the switching of nanopatterned elements, which is a key aspect for MTJ-based probabilistic computing.

KEYWORDS: ferromagnetic disk, patterned arrays, magnetic tunnel junction, magnetization switching, stochastic behavior

Introduction

Stochastic nature in nanomagnetic systems is not only scientifically fundamental for understanding underlying physics of nanospin behavior but also highly relevant to applications of magnetic and spin processes to advanced nanotechnologies.[1-4] Stochastic nature is directly linked to the question of whether the magnetic and spin processes, particularly on a nanoscale is reproducible or not. This issue has been considered to be very crucial mainly from the perspective of securing the accurate performance in magnetic nanodevices.[5-8] Recently, the viewpoint on the stochastic nature in nanomagnetic processes is directed toward a different prospect, *i.e*., harnessing this unique intrinsic phenomenon to probabilistic computing.[9-11]

A promising magnetic system for probabilistic computing based on probabilistic bits (p-bits)[12,13] is magnetic tunneling junction (MTJ) composed of the patterned magnetic elements. Lately, there was an experimental proof-of-concept demonstration on probabilistic computing using MTJs reported by H. Ohno and S. Datta.[14]

To realize computing nanodevices utilizing patterned magnetic units such as MTJ, extensive study on stochastic reversal of individual magnetic elements and their collective nature within arrays is essential, particularly with a perspective that many ensembles or replica of the stochastic building blocks needs to be integrated into a single chipset in real computing applications. Such study is also extremely essential for applications of magnetic elements to high-density data storage and logic applications, for example, magnetoresistance random access memory (MRAM) and nanomagnetic logic. In the applications, reproducibility and controllability of magnetization switching of the individual magnetic elements is a highly desirable feature.[15-17]

So far, most experimental studies on switching processes in magnetic arrays have used macroscopic analytical tools such as assemble-averaged hysteresis loops over large arrays of magnetic disks[18,19] due to limitations in conventional magnetic microscopy techniques. To address the stochasticity issue of the magnetization switching of a single magnetic element in arrays,[20-22] examining individual switching of each magnetic cell with high spatial resolution over a wide field of view (FOV) is highly demanded. However, direct observation of switching behavior of individual patterned elements within an array and the comprehensive understanding the stochasticity in the switching of them have remined elusive. Here, we report the stochasticity of individual switching of $[(Co\ (0.7\ nm)/Pt\ (2\ nm)]_4/Pt\ (5\ nm)$ nanodisks within arrays investigated based on direct imaging by full-field magnetic transmission soft X-ray microscopy (MTXM) and three-dimensional micromagnetic simulations. The disk arrays were fabricated on silicon-nitride (Si_3N_4) membranes by using magnetron sputtering and e-beam lithography (See Scheme 1 and Experimental details).

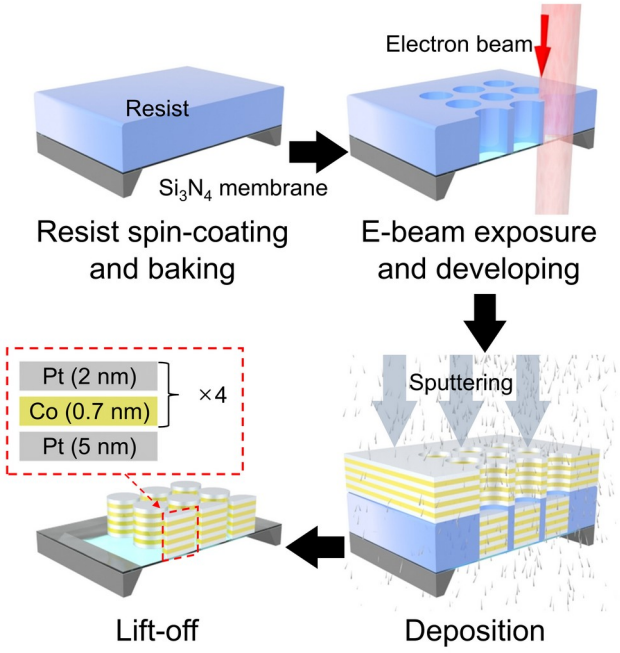

Scheme 1. A schematic diagram of the fabrication process of a [(Co (0.7 nm)/Pt (2 nm)]$_4$/Pt (5 nm) disk array.

Results and Discussion

Images for switching of disks within disk arrays

Figure 1a is a schematic diagram to show the geometry of the disk arrays of a disk radius R ranging from 125 nm to 625 nm, and a constant edge-to-edge distance of 250 nm (See Experimental details). The sample was saturated first by a perpendicular magnetic field of H = +300 mT and the magnetic images were recorded with the magnetic field step of $\Delta H = -1.5$ mT. Figures 1b and 1c show the hysteresis loop and MTXM image of disks with 250-nm radius, respectively. The hysteresis loop was obtained by quantifying the contrast change of MTXM images triggered by the switching of individual disks within the array at each field step. One can note that the disks within the array are not switched coincidentally at a single switching field (H_{sw}). The array of disks shows a distribution in the H_{sw} ranging from −36 mT to −46.5 mT (See Figure 1b). Since the MTXM images in Figure 1c are differential images between sequential field steps, the black contrast corresponds to the magnetization reversal events in individual disks, which occurred at a given magnetic field. The distribution of H_{sw} of 32 disks within the FOV is clearly visualized in the overlapped image with color code indicating the strength of H_{sw} for individual disks and also in the hysteresis loop (See Figure 1b). The H_{sw} distribution of those disks might be due to inhomogeneity of magnetic properties, such as magnetic anisotropy, and/or geometric imperfections associated with edge roughness, which vary from one disk to another.[23,24]

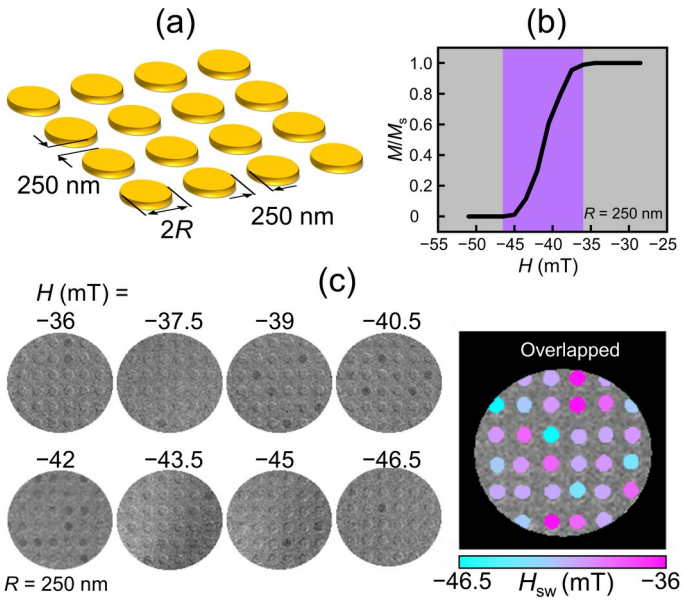

Figure 2. (a) A schematic diagram of circular disks with an edge-to-edge distance of 250 nm. (b) A half hysteresis loop of 250 nm-radius disk array obtained by tracking magnetic contrast change over the array. The purple area indicates the region of magnetization switching occurred in the individual disks. (c) Differential MTXM images of an array of disks with R = 250 nm with sweeping the applied magnetic field, H from −34.5 mT to −45 mT in the field step, ΔH = −1.5 mT. The differential images were obtained by subtracting the image with field, H from the image with the previous field, $H-\Delta H$. An overlapped image of the images showing magnetization reversals of individual disks at different switching fields (H_{sw}) is also added.

Stochasticity in the switching field of disks

To investigate the stochastic behavior of magnetization switching of individual disks, we recorded images in repeated hysteretic cycles in an identical array area. Figures 2a and 2b illustrate MTXM images of an array of disks with R = 250 nm and 625 nm taken respectively at H = −39 mT and +39 mT on the descending and ascending branches of the hysteresis loop in two

consecutive cycles, respectively. Interestingly, in the repeated measurements, the configurations of switched disks are quite different although they are observed at the identical magnetic field.

The inconsistency of the configurations is clearly observable in the combined images of two MTXM images taken at the consecutive measurements, where the red and green represent the disks switched in the first and second cycles, respectively, and the blue indicates the ones reversed in both hysteretic cycles. This result clearly reveals that the switching of individual disks exhibits stochastic nature in repeated hysteretic cycles.

The stochastic H_{sw} can be explained by the thermal fluctuation on the magnetization reversal process of the disk. Since the disk sizes are several hundreds of nanometers, the reversal process proceeds by a domain nucleation, followed by domain wall (DW) propagation. The magnetization reversal of disk is accomplished when the external force exerted by magnetic field exceeds the energy barriers associated with nucleation. Since thermal effect helps to overcome those energy barriers and thus strongly influences the magnetization reversal process, the H_{sw} is expected to fluctuate due to the thermal agitation.[25,26]

The stochasticity in the switching field of individual disks was also identified in the H_{sw} distribution over the large array, as shown in Figure 2c where the configurations of H_{sw} at the identical area of the array taken from 3 repeated measurements are displayed. Figure 2d exhibits the H_{sw} distribution of the array containing 100 disks with R = 250 nm observed in three successive measurements. The distribution noticeably varies in each measurement. The results in Figures 2c and 2d support that the randomly fluctuating H_{sw} of each disk notably affects the H_{sw} distributions over the array and the stochasticity of the magnetization switching in the individual disk could be one of the origins of the change of H_{sw} distribution in large arrays.

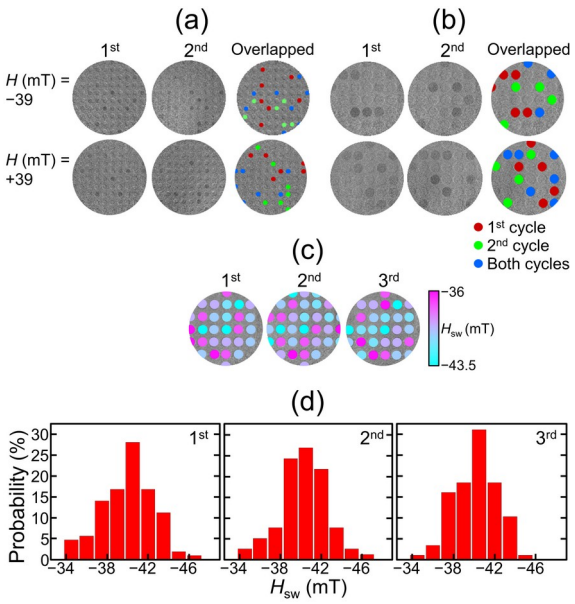

Figure 3. MTXM images of disk arrays with (a) R = 250 nm and (b) 625 nm were taken at H = ±39 mT in two successive hysteretic cycles and their combined images. (c) The repeated measurements for magnetization reversal of the disk array with R = 625 nm at the identical area. (d) Switching field (H_{sw}) distribution over the array containing 100 disks with R = 250 nm observed in three repeated measurements.

Dependency of the stochasticity on the disk size

In various arrays consisting of disks with different sizes of R = 125, 250, 375, 500, and 625 nm, the fluctuation of H_{sw} was systematically investigated. The full hysteretic cycles along the descending and ascending field branches were repeated 50 times and the fields, where the reversal of individual disks occurs, were examined. To quantitatively explore the fluctuation rate of H_{sw} for individual disks, we determined the standard deviation (SD) of H_{sw} taken from 50 repetitions. In each array, the SD of H_{sw} for 25 individual disks was analyzed, which leads to

highly significant statistical ensembles of 1250 in each array. Those SDs of H_{sw} were averaged out to obtain the general value of SD for each array. Figure 3a displays the averaged SD of H_{sw} as a function of the disk radius. We found that the SD considerably depends on the disk size. The SD initially decreases with increasing the disk radius from 125 nm to 375 nm (Region I) and then, the SD increases again as the disk gets bigger from 375 nm to 625 nm (Region II). The trend of SD with respect to the disk size was observed the same in both descending and ascending field branches of the hysteresis loop. The SD of ultra-small disks (R < 125 nm) might show higher SD than those of disks in the Region I of Figure 3a. We found that the averaged H_{sw}, $\langle H_{sw} \rangle$, of arrays consisting of disks with different sizes is rarely varied (Supporting Information).

To interpret the observed result, we investigated the variance of thermal fluctuation given by $V_{ar} = 2\alpha k_b T / (1+\alpha^2)\gamma\mu_0 M_s V$, which is derived from Brown's Fokker-Planck equation,[27] considering that the fluctuation of H_{sw} is attributed to the thermal fluctuation effect on the magnetization switching of disks. γ and α are a gyromagnetic ratio and a damping parameter and V is the island volume, which is the unit volume relevant to thermal stability. Figure 3b shows the relative values of thermal-fluctuation variance with respect to the disk radius, which are calculated with an assumption that the disk volume corresponds to the island volume.

In comparison of the variance of thermal fluctuation and the SD of H_{sw} (Figures 3a and 3b), it is obvious that they show the coincident trend in the Region I, whereas they are countertrends in the Region II. The countertrend between the variance of thermal fluctuation and the SD of H_{sw} observed in larger-sized disks is very interesting since the stochasticity of H_{sw} is expected to be

mainly governed by the degree of thermal fluctuation. The failure of the stochasticity dependency on the thermal-fluctuation variance in larger-sized disk can be attributed to occurrence of different magnetization reversal mechanism as the disks get larger.

Figure 3c shows typical examples of different magnetization reversal types observed in disks with R = 250 and 625 nm in three repeated cycles. The 250-nm radius disk is switched entirely in the field step of ΔH = 1.5 mT as a single island even though it might contain lots of grains with the size of 10 ± 5 nm, which has been measured by XRD in Co/Pt film.[28] In this case, the switching might proceed via the domain nucleation and immediate DW growth without considerable pinning and depinning processes.[29,30] We confirmed that the same reversal behavior of the disk is appeared in the most of hysteretic cycles in the disk array. On the other hand, the 625 nm-radius disk shows different magnetization reversal behavior. Although the disk occasionally reverses like the 250-nm radius disk as shown in the 3rd cycle in Figure 3c, the magnetization reversal of the disk is mostly completed over two field steps, which implies that rather complicate DW pinning and depinning processes may occur during the magnetic reversal of the disks.

The light grey contrast visible in Figure 3c then can be understood to be the existence of intermediate steps in the magnetic switching of the disk through DW pinning and depinning with considering the image acquisition time of several seconds. The multi-step switching is more clearly visible in the differential images between sequential field steps in Figure 3d. The two dark contrasts observed in the 625 nm-radius disk, which are sharply distinguishable from the one dark contrast seen in the one-step switching of the 250 nm-radius disk, clearly reveal two-step switching in the magnetization reversal.

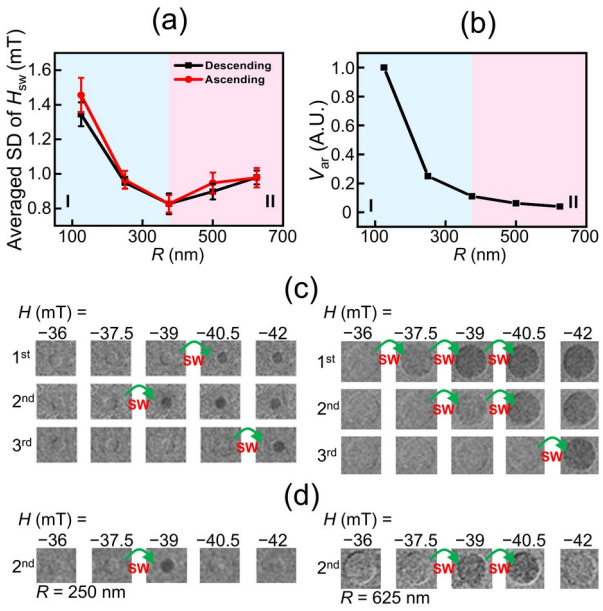

Figure 4. (a) The averaged standard deviation (SD) of switching fields (H_{sw}) of individual disks as a function of the disk radius (R). The averaged value is obtained by statistical analysis of switching events of 25 disks. (b) The relative variances of thermal fluctuation obtained by taking account of the disk volume. (c) MTXM images of magnetization reversal of disks with R = 250 and 625 nm observed in three consecutive measurements in the field step of ΔH = −1.5 mT for a descending branch of the hysteresis loop under identical conditions. (d) Differential MTXM images were obtained by subtracting the image with field, H from the image with the previous field, $H-\Delta H$.

Transformed switching mechanism of disks with varying the disk size

For a more comprehensively understanding the experimentally observed magnetization switching behavior with respect to the disk size, we performed three-dimensional micromagnetic simulations for magnetization reversal dynamic process on individual layers of disks with

polycrystal structure having an average grain size of 10 nm as shown in Figure 4a. Figures 4b and 4c show the dynamic process of magnetization reversal over the four individual layers in the disks of the R = 125 and 375 nm while the external magnetic fields of H = −60.5 and −39 mT are applied, respectively. Interestingly, in both disks, the magnetization switching in individual layers does not occur at once, but it happens through multiple steps by the domain nucleation and propagation on each layer. However, the different switching behavior upon the disk size is clearly observable. For R = 125 nm, the switching starts at the top layer and propagates to the bottom layer during its dynamics, 20 ns. Nevertheless, at the end of dynamic process with the magnetic field of H = −60.5 mT, the magnetization switching over all layers of the disk is completed, which indicates that the switching can be measured as a single island switching under the field sweep with the field step of ΔH = 0.5 mT. This simulation result coincides with the experimental results for the 125 nm-radius disk displayed in Figure 3c. In repeated simulations with a different grain distribution, such single switching was observed all the time in the 125 nm-radius disk, as shown in Supporting Information.

In the magnetization reversal of the larger scaled disk (R = 375 nm), however, different reversal mechanism through the layers was identified in repeated cycles. While the same type of single switching, which is comparable to the case of 125 nm-radius disk (Figure 4b), is also observed in the 375 nm-radius disk at H = −39 mT (Figure 4c), Figure 4d shows that the switching in the 375 nm-radius disk with different grain distribution is completed over two field steps, −39 mT and −40 mT as observed in experiments. At H = −39 mT, only bottom layer is switched. At H = −39.5 mT, the magnetization states were kept without the magnetization switching on the rest three layers. The switching on the rest three layers is completed at H = −40

mT. The different switching mechanism is clearly visualized in the bottom grey-scaled images of disks in Figures 4b-4d. From comparison those simulated images with the MTXM images in Figure 3c, we have successfully measured the transformation of switching mechanism upon the disk size. The layer-by-layer reversal of Co/Pt multilayered disk happens as the disk gets larger.

Note that we also calculated the stray field to investigate the effect of dipolar interaction between nanodisks on the stochasticity in the magnetization switching of the individual disks by micromagnetic simulations (Supporting Information). Based on simulation results showing the increase of stray field as a function of the disk size, which is not consistent with the experimentally observed trend of stochasticity depending on the disk size, we concluded that the dipolar interaction between nanodisks in the arrays would not affect the stochasticity of the magnetization switching of individual disks, especially the dependence on the disk size.

The experiment and simulation results of switching behavior of disks with different disk sizes support that the smaller-sized nanodisks (Region I) can be considered as the single island of which the volume is inversely proportional to the thermal-fluctuation variance as shown in Figures 3a and 3b. Unlike small-sized disks, larger-sized disks (Region II in Figure 3a) are hardly considered as a single unit island directly linked to the thermal-fluctuation variance. As the disk gets larger, the number of local defects increases, resulting in more frequent and complicate DW pinning and depinning events at random positions and more importantly layer-by-layer switching. Note that in those larger disks, DW pinning and depinning processes are still influenced by thermal effect and therefore, such thermally affected DW pinning and depinning processes and layer-by-layer switching would severely contribute to the stochasticity in disk switching, resulting in the high degree of stochasticity in the magnetization switching of larger disks (Region II in Figure 3a).

The presence of the two regions in Figure 3a, which display opposite trends might have an important implication in the use of the magnetic disk array for probabilistic computing. As explicitly shown in Figure 3a, the two competing trends yield the minimized stochasticity at an intermediate disk size, indicating that the stochastic nature of the magnetization switching can be controllable by tuning the size of disks and the switching of disk can be much more optimized for probabilistic computing application.

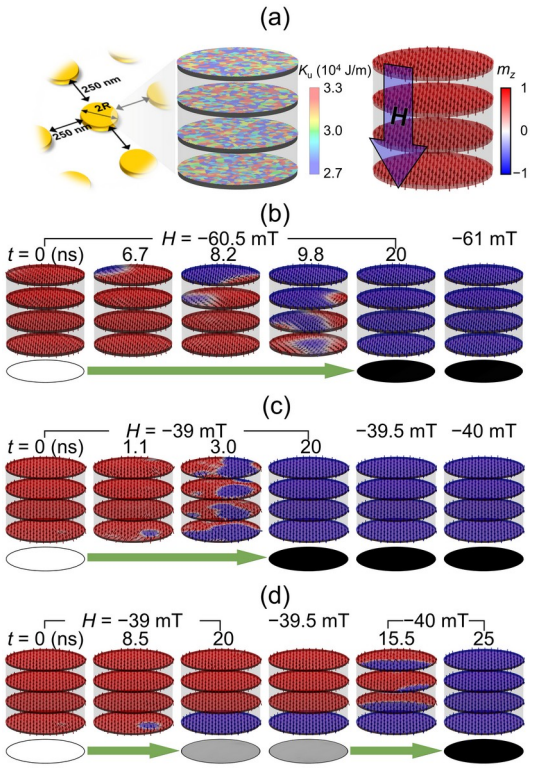

Figure 5. (a) Schematic illustrations of the model system including layout of disk array (left), magnetic grains with different magnetocrystalline anisotropy constant (middle), and the upward out-of-plane initial magnetization (right). (b) Series of snapshot images taken from the micromagnetic simulation of magnetization reversal in a disk of R = 125 nm within array. (c-d) The magnetization switching process with the different magnetic grain in a disk of R = 375 nm

within array. The red and blue colors indicate the upward and downward magnetization, respectively. The grayscale colors represent the simulated MTXM images.

Summary and Conclusion

We have investigated the stochasticity in the magnetization switching of individual [(Co (0.7 nm)/Pt (2 nm)]$_4$/Pt (5 nm) multilayered disks within a large array based on significant statistical measurements utilizing magnetic soft X-ray microscopy. We found that the switching field (H_{sw}) for individual disks stochastically fluctuates within repeated hysteretic cycles and exhibits a decreasing trend in a smaller disk region (125 nm < R < 375 nm) mainly by thermal fluctuations and an increasing trend in a larger disk region (375 nm < R < 625 nm). By performing unique three-dimensional micromagnetic simulation, we demonstrates that the stochasticity depending on the disk size is strongly linked to the transformed magnetization reversal mode, *i.e.*, multi-level layer-by-layer switching. The existence of opposite dependences of stochasticity on the disk size suggests that one can control the stochasticity in the magnetization switching of disks and optimize the design of disk arrays for probabilistic computing. This work provides a scientific insight into stochastic nature in the magnetization switching of nanodisks and an important technological information for their application to probabilistic computing.

Methods

Experimental details

A 5 nm Pt seed layer was grown on the X-ray transparent 200 nm thick Si_3N_4 and subsequently a [(Co (0.7 nm)/Pt (2 nm)]$_4$/Pt (5 nm) multilayer film was deposited using sputtering. The [(Co (0.7 nm)/Pt (2 nm)]$_4$/Pt (5 nm) disks were patterned by electron beam lithography with a disk radius, R ranging from 125 nm to 625 nm and constant edge-to-edge distance of 250 nm. [(Co (0.7 nm)/Pt (2 nm)]$_4$/Pt (5 nm) multilayered film was chosen as its strong perpendicular magnetic anisotropy which provides well-defined and stable magnetic states.[31]

Magnetic structures in the presence of external magnetic fields were recorded at the Co L_3 (778 eV) X-ray absorption edge using MTXM (beamline 6.1.2 at the Advanced Light Source in Berkeley, CA)[32] where the magnetic contrast is obtained using X-ray magnetic circular dichroism (XMCD). The FOV of MTXM and the spatial resolution of MTXM are 10 μm and 25 nm, respectively.

Computational details

Experimental results are complemented by micromagnetic simulations. we used mumax^3 code[33] that numerically solves the Landau-Lifshitz-Gilbert equation $\partial \mathbf{M}/\partial t = -\gamma\mu_0(\mathbf{M}\times\mathbf{H}_{\text{eff}}) + (\alpha/|\mathbf{M}|)(\mathbf{M}\times\partial\mathbf{M}/\partial t)$ with gyromagnetic ratio γ, local magnetization vector $\mathbf{M}$, effective field $\mathbf{H}_{\text{eff}}$ and Gilbert damping constant α[34,35]. As a model system, we assume four-layered [Co (0.7 nm)/Pt (2.1 nm)] circular disks of the radius R = 125 and 375 nm with the cell size 5 × 5 × 0.7 nm^3. To mimic an array system with a 250 nm edge-to-edge distance in our calculations, we used a 2-dimensional periodic boundary condition with 125 nm margin along x and y directions. The simulation parameters for our model system were as

follows: the saturation magnetization M_s = 670 kA/m, exchange stiffness A_{ex} = 14 pJ/m. To explore the magnetization reversal behavior close to a real system, we considered a polycrystal structure in our micromagnetic simulations by assuming a crystalline anisotropy distribution. The grain distribution was constructed using the Voronoi tessellation with average size of 10 nm by referring to the data obtained by X-ray diffraction (XRD) measurements in Co/Pt films and the uniaxial anisotropy constant of K_u = 30 MJ/m^3 was randomly distributed with 10% variation.

ASSOCIATED CONTENT

Supporting Information.

The averaged switching field as a function of the disk size and additional micromagnetic simulation results containing magnetization switching behavior with varying the disk size and grain distribution and the effect of stray field on the magnetization switching in the disk array (PDF).

AUTHOR INFORMATION

Corresponding Authors

Mi-Young Im - Center for X-ray Optics, Lawrence Berkeley National Laboratory, Berkeley, CA, 94720, USA; orcid.org/0000-0002-7346-8152; E-mail: mim@lbl.gov.

Ki-Suk Lee - Department of Materials Science and Engineering, Ulsan National Institute of Science and Technology (UNIST), Ulsan, 44919, Republic of Korea; orcid.org/0000-0002-2063-8007; E-mail: kisuk@unist.ac.kr

Authors

Hee-Sung Han - Center for X-ray Optics, Lawrence Berkeley National Laboratory, Berkeley, CA, 94720, USA; Department of Materials Science and Engineering, Ulsan National Institute of Science and Technology (UNIST), Ulsan, 44919, Republic of Korea; orcid.org/0000-0002-7955-8079.

Sooseok Lee - Department of Materials Science and Engineering, Ulsan National Institute of Science and Technology (UNIST), Ulsan, 44919, Republic of Korea; orcid.org/0000-0002-4812-6302.

Soong-Geun Je - Department of Physics, Chonnam National University, Gwangju 61186, Republic of Korea; orcid.org/0000-0001-9320-0017.

Myeonghwan Kang - Department of Materials Science and Engineering, Ulsan National Institute of Science and Technology (UNIST), Ulsan, 44919, Republic of Korea; orcid.org/0000-0001-5931-3376.

Hye-Jin Ok - Department of Materials Science and Engineering, Ulsan National Institute of Science and Technology (UNIST), Ulsan, 44919, Republic of Korea; orcid.org/0000-0003-3969-4903.

Namkyu Kim - Department of Materials Science and Engineering, Ulsan National Institute of Science and Technology (UNIST), Ulsan, 44919, Republic of Korea; orcid.org/0000-0003-4400-8971.

Weilun Chao - Center for X-ray Optics, Lawrence Berkeley National Laboratory, Berkeley, CA, 94720, USA; orcid.org/0000-0002-9752-370X.

Notes

The authors declare no competing financial interest.

ACKNOWLEDGMENT

Works at the ALS were supported by U.S. Department of Energy (DE-AC02-05CH11231). M.-Y. Im acknowledges support by Lawrence Berkeley National Laboratory through the Laboratory Directed Research and Development (LDRD) Program. This work was supported by the National Research Foundation of Korea (NRF) grant funded by Korea government (MSIT) (NRF-2016M3D1A1027831, NRF-2019K1A3A7A09033400, NRF-2019R1A2C2002996, NRF-

2020R1C1C1006194, and NRF-2020M3F3A2A03082987). This work was also supported by the Research Fund (1.210035.01) of UNIST (Ulsan National Institute of Science and Technology).

REFERENCES

1. Sethna, J. P.; Dahmen, K. A.; Myers, C. R. Crackling noise. *Nature*, 2001, **410**, 242-250.
2. Ryu, K.-S.; Akinaga, H.; Shin, S.-C. Tunable scaling behaviour observed in barkhausen criticality of a ferromagnetic film. *Nat. Phys*., 2007, **3**, 547-550.
3. Im, M.-Y.; Lee, K.-S.; Vogel, A.; Hong, J.-I.; Meier, G.; Fischer, P. Stochastic formation of magnetic vortex structures in asymmetric disks triggered by chaotic dynamics. *Nat. Comm*., 2014, **5**, 5620.
4. Hayward, T. J. Intrinsic nature of stochastic domain wall pinning phenomena in magnetic nanowire devices. *Sci. Rep*., 2015, **5**, 13279.
5. Devolder, T.; Chappert, C.; Katine, J. A.; Carey, M. J.; Ito, K. Distribution of the magnetization reversal duration in subnanosecond spin-transfer switching. *Phys. Rev. B*, 2007, **75**, 064402.
6. Petta, J. R.; Weissman, M. B.; Durin, G. Dependence of Barkhausen pattern reproducibility on hysteresis loop size. *Phys. Rev. E*, 1997, **56**. 2776.
7. Im, M.-Y.; Fischer, P.; Kim, D.-H.; Lee, K.-D.; Lee, S.-H.; Shin, S.-C.; Direct Real-Space Observation of Stochastic Behavior in Domain Nucleation Process on a Nanoscale. *Adv. Mater*., 2008, **20**, 1750.
8. Deutsch, J. M.; Dhar, A.; Narayan, O.; Return to return point memory. *Phys. Rev. Lett*., 2004, **92**, 22.
9. Feynman, R. P. Simulating Physics with Computers, *Int. J. Theor. Phys*., 1982, **21**, 467-488.

10. Kirkpatrick, S.; Gelatt, C. D.; Vecchi, M. P. Optimization by Simulated Annealing, *Science*, 1983, **220**, 671-680.
11. Sutton, B.; Camsari, K. Y.; Behin-Aein, B.; Datta, S. Intrinsic optimization using stochastic nanomagnets. *Sci.* Rep., 2017, **7**, 44370.
12. Camsari, K. Y.; Faria, R.; Sutton, B. M.; Datta, S. Stochastic p-Bits for Invertible Logic. *Phys. Rev. X*, 2017, **7**, 031014.
13. Mizrahi, A.; Hirtzlin, T.; Fukushima, A.; Kubota, H.; Yuasa, S.; Grollier, J.; Querlioz, D. Neural-like computing with populations of superparamagnetic basis functions. *Nat. Comm.*, 2018, **9**, 1533.
14. Borders, W.A.; Pervaiz, A.Z.; Fukami, S.; Camsari, K.Y.; Ohno, H.; Datta, S. Integer factorization using stochastic magnetic tunnel junctions. *Nature*, 2019, **573**, 390.
15. Aign, T.; Meyer, P.; Lemerle, S.; Jamet, J.P.; Ferre, J.; Mathet, V.; Chappert, C.; Gierak, J.; Vieu, C.; Rousseaux, F.; Launois, H.; Bernas; H. Magnetization Reversal in Arrays of Perpendicularly Magnetized Ultrathin Dots Coupled by Dipolar Interaction. *Phys. Rev. Lett*., 1998, **81**, 5656.
16. Chou, S.Y.; Krauss, P.R.; Kong, L.S. Nanolithographically defined magnetic structures and quantum magnetic disk. *J. Appl. Phys*., 1996, **79**, 6101.
17. Im, M.-Y.; Fischer, P.; Han, H.-S.; Vogel, A.; Jung, M.-S.; Chao, W.; Yu, Y.-S.; Meier, G.; Hong, J.-I.; Lee, K.-S. Simultaneous control of magnetic topologies for reconfigurable vortex arrays. *NPG Asia Materials,* 2017, **9**, 348.

18. Hellwig, O.; Berger, A.; Thomson, T.; Dobisz, E.; Bandic, Z.Z.; Yang, H.; Kercher, D.S.; Fullerton, E.E. Separating dipolar broadening from the intrinsic switching field distribution in perpendicular patterned media. *Appl. Phys. Lett*., 2007, **90**, 162516.

19. Hauet, T.; Dobisz, E.; Florez, S.; Park, J.; Lengsfield, B.; Terris, B.D.; Hellwig, O. Role of reversal incoherency in reducing switching field and switching field distribution of exchange coupled composite bit patterned media. *Appl. Phys. Lett*., 2009, **95**, 262504.

20. Engelen, J.B.C.; Delalande, M.; le Febre, A.J.; Bolhuis, T.; Shimatsu, T.; Kikuchi, N.; Abelmann, L.; Lodder, J.C. Thermally induced switching field distribution of a single CoPt dot in a large array. *Nanotechnology*, 2010, **21**, 035703.

21. Shaw, J.M.; Rippard, W.H.; Russek, S.E.; Reith, T.; Falco, C.M. Origins of switching field distributions in perpendicular magnetic nanodot arrays. *J. Appl. Phys*., 2007, **101**, 023909.

22. Lau, J.W.; McMichael, R.D.; Chung, S.H.; Rantschler, J.O.; Parekh, V.; Litvinov, D. Microstructural origin of switching field distribution in patterned Co/Pd multilayer nanodots. *Appl. Phys. Lett*., 2008, **92**, 012506.

23. Thomson, T.; Hu, G.; Terris, B.D. Intrinsic Distribution of Magnetic Anisotropy in Thin Films Probed by Patterned Nanostructures. *Phys. Rev. Lett*., 2006, **96**, 257204.

24. Bryan, M.T.; Atkinson, D.; Cowburn, R.P. Experimental study of the influence of edge roughness on magnetization switching in Permalloy nanostructures. *Appl. Phys. Lett*., 2004, **85**, 3510.

25. Brown, W.F. Thermal Fluctuations of a Single-Domain Particle. *Phys. Rev*., 1963, **130**, 1677.

26. Sharrock, M.P.; McKinney, J.T. Kinetic effects in coercivity measurements. *IEEE Trans. Magn*., 1981, **17**, 3020.

27. Garcia-Palacios, J.L.; Lazaro, F.J. Langevin-dynamics study of the dynamical properties of small magnetic particles. *Phys. Rev. B*, 1998, **58**, 14937.

28. Weller, D.; Notarys, H.; Suzuki, T.; Gorman, G.; Logan, T.; McFadyen, I.; Chien, C.J. Thickness dependent coercivity in sputtered Co/Pt multilayers. *IEEE Trans. Magn*. 1992, **28**, 2500

29. Stoner, E.C.; Wohlfarth, E.P. A mechanism of magnetic hysteresis in heterogeneous alloys *Trans. R. Soc. London A*., 1948, **240**, 599.

30. Hu, G.; Thomson, T.; Rettner, T.; Raoux, S.; Terris, B.D. Magnetization reversal in Co/Pd nanostructures and films. *J. Appl. Phys*., 2005, **97**, 10J702.

31. Lin, C.J.; Gorman, G.L.; Lee, C.H.; Farrow, R.F.C.; Marinero, E.E.; Do, H.V.; Notarys, H.; Chien, C.J. Magnetic and structural properties of Co/Pt multilayers. *J. Magn. Magn. Mater.*, 1991, **93**, 194-206

32. Fischer, P.; Kim, D.-H.; Chao, W.L.; Liddle, J.A.; Anderson, E.H.; Attwood, D.T. Soft X-ray microscopy of nanomagnetism. *Materials Today*, 2006, **9**, 26-33

33. Vansteenkiste, A.; Leliaert, J.; Dvornik, M.; Helsen, M.; Garcia-Sanchez, F.; Van Waeyenberge, B. The design and verification of MuMax3. *AIP Advances*, 2014, **4**, 107133.

34. Landau L.D.; Lifshitz, E. M. On the theory of the dispersion of magnetic permeability in ferromagnetic bodies. *Phys. Z. Sowjetunion*, 1935, **8**, 153.

35. Gilbert, T. L. Lagrangian formulation of the gyromagnetic equation of the magnetization field. *Phys. Rev*., 1955, **100**, 1243.

Table of Contents (TOC)